Optimizing the synthesis of magnesium aluminate spinel by response surface methodology

LIU JIANHUA, LV XIAOJUN*, LAI YANQING, LI JIE, LIU YEXIANG
School of Metallurgy and Environment, Central South University, Changsha [Hunan], China

Synthesis parameters of magnesium aluminate spinel (MAS) were optimized using central composite design (CCD) of response surface methodology (RSM). A quadratic equation model was proposed to describe the corresponding relationships between the spinelisation rate and main factors such as holding time, calcination temperature and mass fraction of $AlCl_3$. The results show that the spinelisation rate of MAS is significantly affected by the mass fraction of $AlCl_3$ and the calcination temperature. The optimum conditions that contribute to the maximum spinelisation rate are as follows: holding time of 189.00 min, calcination temperature of 1143.89 °C and mass fraction of $AlCl_3$ of 5.42 wt.%. The maximum predicted spinelisation rate of MAS is 80.42%, which is consistent with the experimental value of 80.06% under the optimized conditions. It suggests that the regressive equation fits the spinelisation rates perfectly. X-ray diffraction (XRD) result reveals that MAS is synthesized by solid-state reaction. $AlCl_3$ addition can enhance the formation of MAS from alumina and magnesia without any contamination.

(Received November 21, 2014; accepted August 3, 2016)

Keywords: Magnesium aluminate spinel, Spinelisation rate, $AlCl_3$, Response surface methodology

1. Introduction

Magnesium aluminate spinel (MAS) has a cubic structure which can be viewed as a combination of the rock salt and zinc blende structure [1]. Due to the stable structure, MAS offers a unique combination of desirable properties - chemical stability, thermal shock resistance, corrosion resistance and excellent high temperature mechanical properties [2-4]. Consequently, MAS has been used for various application fields, such as refractories, transparent ceramic materials, humidity sensors and anode materials [5-8].

However, MAS has not been commercially produced in large scale due to the difficulty in sintering [9]. This is mainly because of the volume expansion (about 5%) during the formation of spinel from magnesia and alumina [10,11]. Therefore, the material could not be densified through a single stage firing. Hence a double stage firing process is employed to avoid this problem. In double stage firing process, the raw materials is firstly calcined at around 1400 °C to complete the spinelisation process, and then sintered to achieve densified MAS [12,13]. The greater spinelisation rate of MAS in the first firing process is beneficial to relieve the adverse effect of the volume expansion of MAS in the second sintering process. Therefore, it is important to investigate the influence of different synthesis factors on the spinelisation rate of MAS and further optimize the synthesis parameters.

Previous studies [14-16] proved that the calcination temperature, holding time, additives showed significant influence on the synthesis of MAS. It was demonstrated that high calcination temperature, long holding time and additive was beneficial to enhance spinelisation rate. It was reported that the $AlCl_3$ addition promoted the synthesis of MAS [17]. However, the influence of $AlCl_3$ content on the spinelisation rate of MAS remains open. Until now, the conventional practice does not point out the combined effect of these process parameters (such as calcination temperature, holding time and $AlCl_3$ content) on the spinelisation rate of MAS. To solve the problem, it is necessary to find multivariate statistic techniques to optimize the preparation processes.

In the present work, the effect of $AlCl_3$ addition on the spinelisation rate of MAS was investigated. In consideration of the combined effect of mass fraction of $AlCl_3$, calcination temperature and holding time, responding surface methology was applied to explore the influence of these factors on the spinelisation rate of MAS. The optimum synthesis parameter was obtained through the CCD of RSM.

2. Experimental

The raw materials for the study were high pure alumina and magnesium hydroxide. Raw materials were characterized in terms of chemical analysis by standard wet chemical method and phase identification by X-ray diffraction study. Chemical and phase composition of the raw materials is listed in Table 2. The raw materials were dried for 48 h at 120 °C before being used. Batch composition was made from the raw materials. The MgO:

Al_2O_3 molar ratio was set as 1:1. Anhydrous $AlCl_3$ was added into the above mixture with concentration ranges from 0.636 to 7.364 % (mass fraction). All the batches were individually attrition milled with isopropanol for 3 h by using a zirconia pot and zirconia grinding media. The obtained slurry was initially air dried and subsequently oven dried at 120 °C, then the dried slurry was crushed and put through graded sieves (40 mesh) to get the desired powders. These powders were mixed with 5% PVA solution as binder and uniaxially pressed at 10 MPa on hydraulic press into cylindrical bars.

The calcination experiments were carried out at different calcination temperature, holding time and mass fraction of $AlCl_3$. Cylindrical bars were dried at 120 °C and then calcinated at different calcination temperature in a programme controlled electric furnace. Heating rate was maintained at 3 °C/min up to the final temperature with a holding time at the peak temperatures. They were air cooled to room temperature.

Cylindrical bars were crushed and put through graded sieves (40 mesh) to get the calcinated powders. The spinelisation rate of MAS was determinated by conventional acid dissolution methods.(conventional acid dissolution methods —leaching of the powder samples in 3 mol/dm^3 HCl and determination of the concentration of Mg^{2+} ion in the solution by titration with chelaton III) [18]. Phase analysis of the raw materials and calcinated powders was carried out by X-ray diffraction (Japan Rigaku D/Max-2400) using Cu-Kα radiation. These powders were scanned in the angular range from 15 ^{o} to 80 ^{o} (2θ) with scanning rate 0.005 ^{o}/s .

The three variable and two 1evel CCD was employed to optimize the synthesis condition of MAS in order to obtain a high spinelisation rate. This method helped to optimize the effective parameters with a minimum number of experiments and also analyzed the interaction between the parameters and results [19]. The three independent variables were holding time (x_1), calcination temperature (x_2) and mass fraction of $AlCl_3$ (x_3), respectively. Both coded and actual values of the independent variables investigated in this design are listed in the Table 1.

Table 1. Independent variables and their levels used for CCD

Independent variable	Levels				
	-1.682	-1	0	1	1.682
Holding time (x_1) /*min*	130	150	180	210	230
Calcination temperature (x_2) /*°C*	1016	1050	1100	1150	1184
Mass of fraction $AlCl_3$ (x_3)/*wt.%*	0.636	2	4	6	7.364

To predict the optimal point, a second-order polynomial function was used to fit the correlation between the independent variables and the response on the basis of the above design. The recommended quadratic model was as follows [20]

$$Y = \beta_0 + \sum \beta_i x_i + \sum \beta_{ii} x_i^2 + \sum \beta_{ij} x_i x_j \quad (1)$$

where Y is the predicated response; β_0 is the interception coefficient; β_i are the linear terms; β_{ii} are the quadratic terms; β_{ij} are the interaction terms, and x_i and x_j are the coded levels of the independent variables.

3. Results and disscusion

Physicochemical properties of the raw materials alumina and magnesium hydroxide are given in Table 2. It can be seen from the Table 2 that the alumina consists of 99.12 wt-% Al_2O_3 and the magnesium hydroxide contains $Mg(OH)_2$ of 98.19 wt-%. X-ray analysis of raw materials indicates that the mineralogical phases present in the raw materials are corundum (α-Al_2O_3) and brucite. No minor phases are detected.

Table 2. Physicochemical properties of raw materials

	Al_2O_3	$Mg(OH)_2$
Chemical analysis		
SiO_2	0.38	0.66
Al_2O_3	99.12	Trace
Na_2O	0.11	0.19
MgO	Trace	67.72
CaO	0.14	0.83
Fe_2O_3	0.25	0.13
Phase analysis	corundum	brucite

Effects of the holding time (x_1), calcination temperature (x_2) and mass fraction of $AlCl_3$ (x_3) on spinelisation rate are investigated. The results of 20 runs using CCD are given in the Table 3, which shows that the spinelisation rates of MAS range from 63.90% to 80.21%.

Table 3. CCD arrangement and results

Run	x_1/min	x_2/°C	x_3 /wt.%	Y/%
1	150	1050	2	63.90
2	210	1050	2	64.61
3	150	1150	2	74.22
4	210	1150	2	79.52
5	150	1050	6	72.32
6	210	1050	6	74.78
7	150	1150	6	78.66
8	210	1150	6	80.21
9	130	1100	4	71.34
10	230	1100	4	72.46
11	180	1016	4	70.43
12	180	1184	4	79.52
13	180	1100	0.636	72.76
14	180	1100	7.364	80.20
15	180	1100	4	76.15
16	180	1100	4	77.17
17	180	1100	4	76.56
18	180	1100	4	77.09
19	180	1100	4	77.11
20	180	1100	4	76.72

The experimental data are analyzed using analysis of variance (ANOVA) to assess the goodness of fit, which are listed in Table 4. Generally the ANOVA and *P*-value are used to check the significance of each cocfficient and indicate the interaction strength of each parameter.

It can be seen from Table 4 that the model is actually significant, which indicates that the model is suitable for this experiment. The *F*-value of 18.43 and *P*-value less than 0.0001 demonstrate that this regression is statistically significant at 99% confidence level. Besides, coefficient of determination (R^2) is 0.9432, proving that the model is effective. In addition, the adjusted coefficient of determination (R_{Adj}^2) is 0.892. It implies that the accuracy and general availability of the polynomial model are adequate. Multivariable linear regression is used to calculate the coefficients of second-order polynomial equation and obtain regression coefficients. In the present experiment, the x_2, x_3, and the interaction terms (x_2x_3, x_1^2) are significant model terms whereas the other terms are insignificant to the response.

Data obtained from the experiments was analyzed by linear multiple regression software. The corresponding second-order response model for Eq. (1) established after analysis for the regression is:

$$Y = 76.83 + 0.87x_1 + 3.83x_2 + 2.65x_3 + 0.46x_1x_2 - 0.25x_1x_3 - 1.68x_2x_3 - 1.9x_1^2 - 0.81x_2^2 - 0.28x_3^2 \quad (2)$$

Where Y is the response of spinelisation rate, x_1 is the coded values of holding time, x_2 is the coded values of calcination temperature, x_3 is the coded values of mass fraction of $AlCl_3$.

Table 4. ANOVA for response surface quadratic model analysis of variance

Source	Sum of Squares	df	Mean Square	F	P-value (Prob.>F)	
Model	389.14	9	43.24	18.43	<0.0001	Significant
x_1	10.38	1	10.38	4.42	0.0617	
x_2	200.19	1	200.19	85.35	<0.0001	
x_3	96.13	1	96.13	40398	<0.0001	
x_1x_2	1.69	1	1.69	0.72	0.4155	
x_1x_3	0.50	1	0.50	0.21	0.6542	
x_2x_3	22.65	1	22.65	9.66	0.0111	
x_1^2	51.94	1	51.94	22.15	< 0.0008	
x_2^2	9.49	1	9.49	4.04	< 0.0720	
x_3^2	1.12	1	1.12	0.48	< 0.5046	
Residual	23.46	10	2.35			
Lack of Fit	22.66	5	4.53	28.53	0.0011	Significant
Pure Error	0.79	5	0.16			
Cor. Total	412.59	19				

R^2=0.9432, R_{Adj}^2=0.8920, R_{pred}^2=0.5658, Adequate precision=14.737

The best way to visualize the influence of the independent variables on the response is to draw surface response plots of the model [21]. The spinelisation rate of MAS with different combinations of independent variables is visualized through three-dimensional (3D) view of response surface plot (Figs. 1-2).

The effects of calcination temperature and holding time on spinelisation rate of MAS are given in Fig. 1 with the fixed $AlCl_3$ mass fraction of 4 wt-%. It is observed that the spinelisation rate significantly increases with increasing calcination temperature.

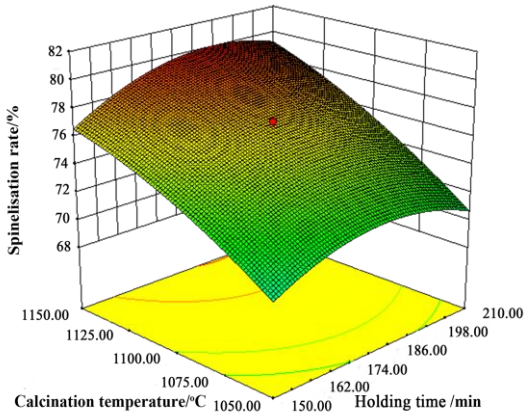

Fig. 1. 3D response surface of calcination temperature vs. holding time on spinelisation rate

According to $MgO\text{-}Al_2O_3$ phase diagram [22] and Wagner mechanism [9], the formation of MAS phase is achieved through mutual transfer of Al^{3+}/Mg^{2+} into solid-state MgO/Al_2O_3 respectively [23]. An increase in calcination temperature will lead to an increase in the spinelisation rate of MAS. In other word, the increase in calcination temperature has sufficient energy for solid-state reaction to occur.

The effects of the mass fraction of $AlCl_3$ and holding time on spinelisation rate of MAS are given in Fig. 2 with the fixed calcination temperature of 1100 °C. Fig. 2 shows that the spinelisation rate increases with increasing mass fraction of $AlCl_3$.

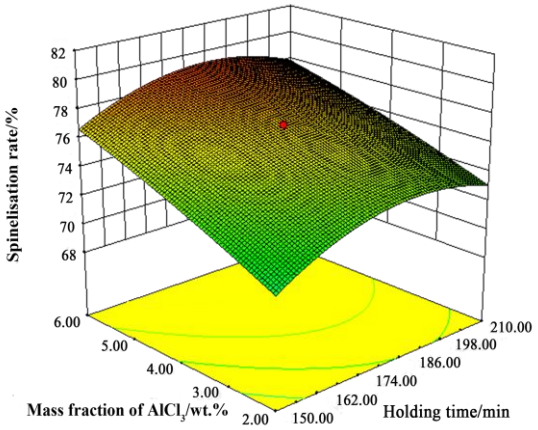

Fig. 2. 3D response surface of mass fraction of $AlCl_3$ vs. holding time on spinelisation rate

As the thickness of spinel increases, the spinel layer breaks direct contact between MgO and Al_2O_3 increasing resistance to diffusion. According to $AlCl_3$ and AlF_3 have the same machanism [17]. F^- ions from mineralizers such as AlF_3 and CaF_2 increase cation vacancy levels when substituting for oxide ions and thus enhance solid state reaction to produce MAS[24]. Fig. 3 illustrates the mechanism of Cl^- ion schematically at the Al_2O_3/spinel boundary.

Initially, the Cl^- ion can incorporate in the anion sublattice during the calcination. The concentration of Mg^{2+} vacancies within $MgAl_2O_4$ can be increased. This could promote the movement of Mg^{2+} through the $MgAl_2O_4$ lattice easier. Then Cl^- ion is easy to escape from the sample surface due to pyrolysis and gasification mechanism. The concentration of Cl^- ion on the sample surface is reduced. So Cl^- ion within the grain diffuses to the surface. The Cl^- ion can escape faster with increasing calcination temperature. In addition, according to the electrostatic interaction, Mg^{2+} transfer into the solid-state Al_2O_3 after the Cl^- ion incorporates in the anion sublattice. Diffused Mg^{2+} reacts with Al_2O_3 to form $MgAl_2O_4$ at the Al_2O_3/spinel boundary ($3\ Mg^{2+} + 4\ Al_2O_3 = 3\ MgAl_2O_4 + 2\ Al^{3+}$).

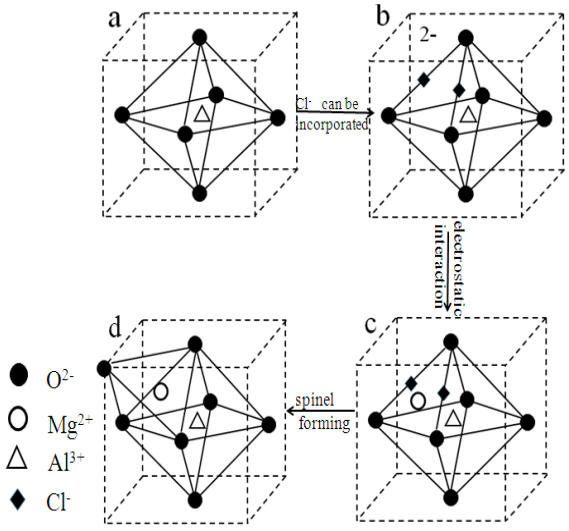

Fig. 3. The schematic diagram illustrating the mineralizing mechanism of Cl^- ion at the Al_2O_3/spinel boundary:(a) Al_2O_3 lattice; (b) electronegative Al_2O_3 lattice forming by incorporated Cl^- ion; (c) Mg^{2+} diffusion at Al_2O_3/spinel boundary by electrostatic interaction; (d) spinel forming on the alumina surface by solid-state reaction.

Predicted and experimental value of the responses at optimun conditions are given in Table 5. The predicted spinelisation rate of MAS under optimum conditions is obtained through point prediction method and surface response plot. The experimental value is compared with predicted one in order to evaluate the validity of the model.

Table 5. Predicted and experimental value of the responses at optimun conditions

Holding time /*min*	Calcination temperature / ℃	Mass fraction of $AlCl_3$ /*wt.%*	Spinelisation rate /%	
			Predicted value	Experimental value
189.00	1143.89	5.42	80.42	80.06

From the Table 5, the optimal conditions are as follows: holding time of 189.00 min, calcination temperature of 1143.89 °C and mass fraction of $AlCl_3$ of 5.42 wt-%. The predicted value of spinelisation rate is 80.42%. The experimental value of that under these conditions is 80.06%, It indicates that the experimental value is in agreement with predicated one.

Phase analysis of calcinated powders and dried powders is shown in Fig. 4. The peaks of MAS, together with corundum and periclase, are visible.

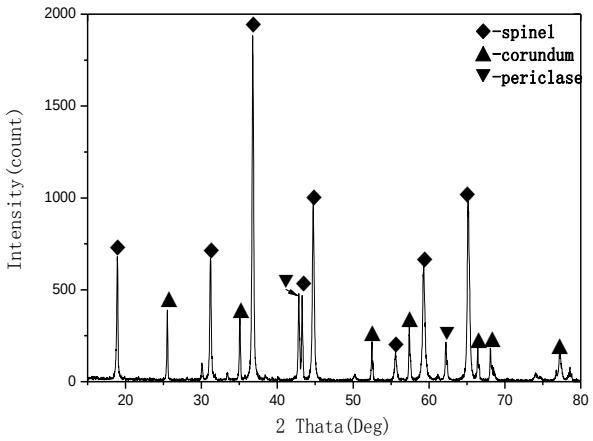

Fig. 4. XRD patterns of calcined powders under optimization conditions

According to the results of the XRD analysis (Fig.4), Magnesium aluminate spinel, together with corundum and periclase, is obtained by calcination under optimization conditions. MgO, resulted from the dissociation of $Mg(OH)_2$, reacts with α-Al_2O_3 to form MAS. Thus, it is feasible to obtain greater spinelisation rate of MAS by cakcination under optimum conditions. On the other hand, the X-ray diffraction peaks of $AlCl_3$ and other chloride are absent. It is possible that $AlCl_3$ is hydrolyzed into Al_2O_3 and gaseous HCl (evaporated) during calcination. Therefore, $AlCl_3$ addition does not contaminate the MAS product.

4. Conclusions

(1) The spinelisation rate of MAS is significantly affected by calcination temperature and mass fraction of $AlCl_3$ compared with the holding time at the calcination temperature.

(2) The optimized calcination condition is as follows: holding time of 189.00 min, calcination temperature of 1143.89 °C and mass fraction of $AlCl_3$ of 5.42 wt-%. Under the optimized condition, the obtained experimental spinelisation rate of MAS (80.06%) is found to agree satisfactorily to the predicted value of 80.42%. It suggests that RSM and CCD are appropriate for determining the optimal conditions for spinelisation process of MAS to obtain the maximum spinelisation rate.

(3) The $AlCl_3$ addition is beneficial to promoting the formation of MAS from alumina and magnesia devoid of any contamination.

Acknowledgement

This work was supported by National Natural Science Foundation of China (No. 51204211).

References

[1] W. D. Kingery, H. K. Bowen, D. R. Uhlman. A Wiley-interscience Publication, Massachusetts 63 (1976).
[2] C. Baudin, R. Martinez, P. Pena. J. Am. Ceram. Soc. **78,** 1857 (1995).
[3] E. Ruh, Am. Ceram. Soc. Bull. **63,** 1140 (1984).
[4] I. Ganesh, S. Bhattacharjee, B. P. Saha, et al. Ceram. Int. **28,** 245 (2002).
[5] R. D. Maschio, B. Fabbri, C. Fiori. Ind. Ceram. **8,** 121 (1988).
[6] Y. Shimizu, H. Arai, T. Seiyama, Sensors Actuators **7,** 11 (1985).
[7] L. Ji-Guang, T. Ikegami, L. Jong-Heum, et al. J. Am. Ceram. Soc. **83**, 2866 (2000).
[8] S. Angappan, L. J. Berchmans, C. O. Augustin, Mater. Lett. **58,** 2283 (2004).
[9] I. Ganesh. Int. Mater. Rev.**58,** 63 (2013).
[10] R. Naghizadeh, H. R. Rezaie, F. Golestani-Fard, Ceram. Int. **37**, 349 (2011).
[11] E. Ryshkewitch, Academic Press, New York, 257 (1960).
[12] R. E. Carter, J. Am. Ceram. Soc.**44 ,** 116 (1961).
[13] H. S. Tripathi, Ceram. Int.**36,** 1189 (2010).
[14] H. S. Tripathi, B. Mukherjee, S. Das, et al. Ceram. Int.**29,** 915 (2003).
[15] T. Noda, S. Hasegawa. J. Soc. Chem. Inds., Japan **43,** 169 (1940).
[16] W. T. Baker, J. G. Lindsay. Am. Ceram. Soc. Bull. **46,** 1094 (1967).

[17] I. Ganesh, S. Bhattacharjee, B. P. Saha, et al. Ceram. Int. **27,** 773 (2001).
[18] B Plešingerová, N Števulová, M Luxova, et al. Journal of Materials Synthesis and Processing **8,** 287 (2000).
[19] R. Azargohar, A. K. Dalai. Micropor. Mesopor. Mater. **85,** 219 (2005).
[20] N. F. Zainudin, K. T. Lee, A. H. Kamaruddin, et al. Sep. Purif. Technol. **45**, 50 (2005).
[21] C. John, W. Cleveland, B. Kleiner, et al. Wadsworth, Ohio128 (1983).
[22] B. Hallstedt, J. Am. Ceram. Soc. **75,** 1497 (1992).
[23] Ritwik Sarkarn, Sachin Sahoo. Ceram. Int. **40,** 16719 (2014).
[24] E. Kostic, S. Bokovic, S. Kis, J. Mater. Sci. Lett. **1,** 507 (1982).

*Corresponding author: csuxiaojun@126.com